RESEARCH ARTICLE

Re-emergent Tremor in Parkinson's Disease: Evidence of Pathologic β and Prokinetic γ Activity

Hao Ding, PhD,[1,2] Bahman Nasseroleslami, PhD,[2] Daniela Mirzac, MSc,[3] Ioannis Ugo Isaias, MD, PhD,[1] Jens Volkmann, MD, PhD,[1] Günther Deuschl, MD,[4] Sergiu Groppa, MD, PhD,[3] and Muthuraman Muthuraman, PhD[1*]

[1]*Department of Neurology, University Hospital Würzburg, Würzburg, Bavaria, Germany*
[2]*Academic Unit of Neurology, Trinity College Dublin, the University of Dublin, Dublin, Leinster, Ireland*
[3]*Department of Neurology, University Medical Center of the Johannes Gutenberg-UniversityMainz, Mainz, Rheinland-Pfalz, Germany*
[4]*Department of Neurology, UKSH, Christian-Albrechts-University Kiel, Kiel, Schleswig-Holstein, Germany*

ABSTRACT: Background: Re-emergent tremor is characterized as a continuation of resting tremor and is often highly therapy refractory. This study examines variations in brain activity and oscillatory responses between resting and re-emergent tremors in Parkinson's disease.
Methods: Forty patients with Parkinson's disease (25 males, mean age, 66.78 ± 5.03 years) and 40 age- and sex-matched healthy controls were included in the study. Electroencephalogram and electromyography signals were simultaneously recorded during resting and re-emergent tremors in levodopa on and off states for patients and mimicked by healthy controls. Brain activity was localized using the beamforming technique, and information flow between sources was estimated using effective connectivity. Cross-frequency coupling was used to assess neuronal oscillations between tremor frequency and canonical frequency oscillations.
Results: During levodopa on, differences in brain activity were observed in the premotor cortex and cerebellum in both the patient and control groups. However, Parkinson's disease patients also exhibited additional activity in the primary sensorimotor cortex. On withdrawal of levodopa, different source patterns were observed in the supplementary motor area and basal ganglia area. Additionally, levodopa was found to suppress the strength of connectivity ($P < 0.001$) between the identified sources and influence the tremor frequency-related coupling, leading to a decrease in β ($P < 0.001$) and an increase in γ frequency coupling ($P < 0.001$).
Conclusions: Distinct variations in cortical–subcortical brain activity are evident in tremor phenotypes. The primary sensorimotor cortex plays a crucial role in the generation of re-emergent tremor. Moreover, oscillatory neuronal responses in pathological β and prokinetic γ activity are specific to tremor phenotypes. © 2024 The Authors. *Movement Disorders* published by Wiley Periodicals LLC on behalf of International Parkinson and Movement Disorder Society.

Key Words: cerebello-cortical circuits; pathological neuronal oscillatory activity; tremor-related phenotype

*__Correspondence to:__ Dr. Muthuraman Muthuraman, Department of Neurology, University hospital Würzburg, Würzburg, Bavaria, 97080, Germany; E-mail: muthuraman_m@ukw.de

Relevant conflicts of interest/financial disclosures: None.

Funding agencies: This work was supported by the German Research Foundation (DFG): SFB-TRR-295 (to M.M.), MU 4354/1-1 (to M.M.), and the Fondazione Grigioni per il Morbo di Parkinson by IUI.

Received: 12 September 2023; **Revised:** 15 February 2024; **Accepted:** 20 February 2024

Published online 26 March 2024 in Wiley Online Library (wileyonlinelibrary.com). DOI: 10.1002/mds.29771

Parkinson's disease (PD) is characterized by a variety of symptoms, with tremor being one of the cardinal signs. Tremor is a highly heterogeneous symptom, ranging from mild to severe manifestations, and presenting as rest, postural, and kinetic tremor.[1] Resting tremor (RT) in PD is commonly described as asymmetric, with a frequency of 4 to 6 Hz, and typically involves the hands in a pill-rolling pattern.[2,3] The inhibition of tremor during voluntary movements is a characteristic of the RT in PD.[4] However, tremor can re-emerge during stable posture or actions after a brief latency, a phenomenon known as re-emergent tremor (RET). Because it shares similar frequency characteristics with RT,[5] it was proposed to be the "continuation" of RT.[6]

One model of tremor pathology suggests that the basal ganglia (BG) act as a "light-switch" for motor activity, initiating tremor episodes, whereas the cerebello-thalamo-cortical circuit functions as a "light-dimmer," modulating tremor rhythm.[1] Within this circuit, the motor cortex determines the tremor amplitude, whereas the thalamus and cerebellum (CER) may maintain the tremor rhythm.[7] Previous studies have shown that there are common pathophysiological mechanisms for both RT and RET, in which the motor cortex plays an important role.[8] However, a less responsiveness of dopamine was found in RET.[6] More recently, transcranial magnetic stimulation at CER was shown to reset RET, but not RT.[9] These findings suggest that the two tremor types exhibit differences in their common pathophysiological mechanisms and involve non-dopaminergic areas such as the CER during RET.

Within the cerebello-cortical network, the sensorimotor cortex (SMC), premotor cortex (PMC), and supplementary motor areas (SMA) have demonstrated distinct roles in tremor phenotypes between RT in PD and mimicked tremor in healthy individuals.[10,11] Based on the frequency of tremor, cerebro-cerebral coherence analysis has revealed a widespread network connected to the M1, including the SMA and lateral PMC.[12] Although the cerebello-thalamo-cortical circuit is responsible for sustaining the tremor,[7] periods of the tremor were found to be associated with enhanced synchronization of low β power in the PMC.[13] These findings underscore the involvement of these motor regions in the mechanism of tremor and suggest a potential role in bridging the gap between RT and RET.

Building on prior research, this study posits that specific motor regions and CER are implicated in cortico-subcortical communication differences between RT and RET during stable posture in PD. To achieve this, the study analyzed simultaneously acquired high density electroencephalography (EEG)–electromyography (EMG) signals from PD patients during RT and RET. It used structural magnetic resonance imaging (MRI) and EEG in tandem with EMG to identify brain activity differences between RT and RET. Effective connectivity were estimated between identified source regions. We further investigated oscillatory coupling between the differentiated tremor power from cortical source regions and canonical frequency bands from subcortical source regions. By integrating multimodal datasets, this study has the potential to reveal significant findings on the underlying networks involved in RT and RET (Fig. 1).

Materials and Methods

Study Participants and Experiment Procedures

This study included 40 patients (66.78 ± 5.03 years old, 15.25 ± 2.72 disease duration) who were clinically

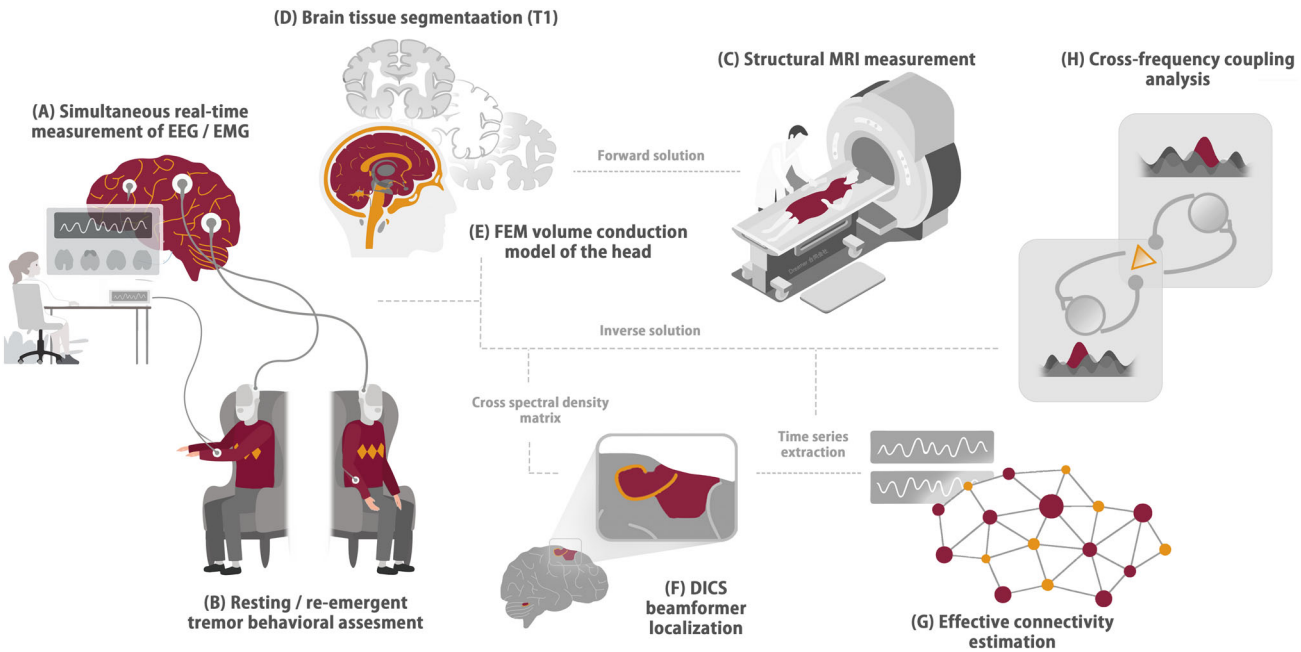

FIG. 1. Schematic of experiment and analysis pipeline. (**A**) EEG–EMG measurements were simultaneously recorded from the participants. (**B**) PD patients performed both resting and re-emergent tremors during the measurement, whereas healthy participants mimicked the two tremor types. (**C**) All participants underwent structural MRI acquisition. (**D**) Brain tissue segmentation performed based on the T1 image. (**E**) Realistic head model construction performed using the FEM method. (**F**) DICS technique used for source localization. (**G**) Effective connectivity estimation applied to the time series extracted from the coherent source. (**H**) Cross-frequency coupling analysis performed on the time series extracted from the coherent source. DICS, dynamic imaging of coherent sources; EEG, electroencephalography; EMG, electromyography; FEM, finite element method; MRI, magnetic resonance imaging; PD, Parkinson's disease. [Color figure can be viewed at wileyonlinelibrary.com]

diagnosed with definite PD according to the London Brain Bank criteria.[14] The inclusion criteria required the presence of RT with a summed score for amplitude and constancy reaching at least four. Additionally, the RET was assessed with a variable delay after participants held their arm outstretched, requiring an amplitude score of at least two based on Unified Parkinson's Disease Rating Scale (UPDRS) rating on the dominant arm, and a frequency similar to that of RT. The exclusion criteria encompassed a history of other neurological or psychiatric conditions, advanced PD (Hoehn and Yahr scale >4),[15] or the presence of head tremor. A control group of 40 age- and sex-matched volunteers (65.78 ± 2.72 years) with normal neurological exams was also included. All participants gave written consent, and the study was approved by the institutional review board in accordance with the Declaration of Helsinki.

All PD participants underwent measurements 3 hours after medication intake. Among them, 19 individuals participated in measurements under medication-off conditions, following an overnight withdrawal. During the experiment, participants were seated in a comfortable armchair, providing forearm support for optimal EEG–EMG measurement with surface electrodes during tremor. The experimental protocol comprised a 1-minute resting state with eyes open, followed by an instruction to hold their arms outstretched for 1 minute, with their gaze fixed on a point located 2 m away. This sequence was repeated across a series of 10 trials for each participant.

Healthy participants simulated RT by executing fast rhythmic extension-flexion arm movements and replicated RET tremor as instructed, mirroring the behavior observed in PD patients. They produced the movements at their own pace while their EMG activity was monitored for consistency. Frequencies below two to five bursts per second were discarded. The participants who could not sustain the movements for more than 1 minute repeated the task.

EEG–EMG Data Acquisition and Preprocessing

A high-density 256-channel recording system was used to record EEG data. EMG data were simultaneously recorded using silver-silver chloride electrodes from the forearm flexors and extensors. Data acquired from the dominant side was used for further analysis. Raw EEG and EMG signals were recorded at a sampling rate of 1000 Hz and band-pass filtered (EMG, 30–200 Hz; EEG, 0.05–200 Hz). Full-wave rectification of the EMG signal was performed before filtering to produce demodulated EMG.[16] Each recording was segmented into 1-second epochs, and any data segments with visible artefacts were discarded.

Coherence and Time-Frequency Analysis

Cortico-muscular coherence was calculated to determine the time-interval of interest for subsequent source estimation. We computed the EEG–EMG coherence spectrum using the Welch periodogram method.[17] The spectral coherence was calculated as shown in Equation (1):

$$C_{\mathrm{EEG-EMG}}(f) = \frac{|S_{\mathrm{EEG-EMG}}(f)|^2}{S_{\mathrm{EEG}}(f) S_{\mathrm{EMG}}(f)}, \quad (1)$$

where $S_{\mathrm{EEG\text{-}EMG}}$ represents the cross-spectral density (CSD) between activity at the EEG electrode and EMG. S_{EEG} and S_{EMG} are the auto spectral densities. Coherence is calculated in the frequency domain by normalizing the magnitude of the combined CSD between EEG and EMG signals by their respective power. Each coherence value for a frequency bin is a number ranging from 0 to 1. To assess the statistical significance of coherence at a specific frequency, we used the formula $1-(1-x)^{1/(M-1)}$, with x set to 0.99.[18] This establishes a confidence limit of $1-0.01^{1/(M-1)}$. Coherence values surpassing this limit indicate a correlation between the two-time series, whereas values below it suggest no correlation.

Furthermore, we used the multitaper method.[19] This involved estimating the spectrum by applying K distinct windows ($K = 7$) to the data $x(t)$.[10,20] We used overlapping windows of 1000 ms with a time step of 50 ms, yielding an approximate frequency resolution of 1 Hz and time resolution of 50 ms. We computed an initial coherence estimate for each individual EEG electrode.[21,22] Subsequently, the coherence estimates originating from EEG electrodes that displayed significant coherence with EMG were aggregated to a pooled coherence estimate. This was done by combining individual second-order spectra through a weighting scheme as previously described.[21,22] Based on the pooled time-frequency spectrum, we selected the time intervals per each trial that showed significant coherence between the EEG and EMG signals at the tremor frequency.

Cortico-Muscular Coherent Sources Localization

We created a realistic head model, including individual electrode locations, head geometry, and conductivity, using a finite-element method based on T1 images with compartments. This model enabled precise forward problem computations of EEG potentials in subsequent analyses. We solved the EEG source localization using the dynamical imaging of coherent sources beamforming technique,[23,24] which applies a spatial filter[25] to compute tomographic maps of

cerebro-muscular coherence. We analyzed RT and RET recordings separately and compared the difference between the two conditions. The spatial filter was used across numerous voxels in these areas, assigning coherence value to each voxel with a granularity of 2 mm. The regions that showed the strongest coherence to the EMG signal at the tremor frequency were identified as the source. The individual maps were normalized and averaged. For left-handed participants, individual maps on the contralateral hemisphere were flipped before averaging. The resulting maps were displayed on a standard Montreal Neurological Institute template brain, with local maxima representing the strongest coherence to the EMG signal. The time series from the sources were extracted for connectivity analysis.

Effective Connectivity Estimation

To assess directed connectivity at a specific frequency, we used the time-resolved partial directed coherence (TPDC) method. TPDC has been widely used in previous studies analyzing time series data such as EEG, EMG, and magnetoencephalogram,[26,27] owing to its ability to disregard indirect influences. This approach uses the dual-extended Kalman filter[28] to estimate the time-dependent autoregressive coefficients, which are then subjected to Fourier transformation to calculate partial directed coherence (PDC).[29] PDC between time series x_j and x_i at each time point can be determined by:

$$\pi_{i\leftarrow j}(f) = \frac{|A_{ij}(f)|}{\sqrt{\sum_{k=1}^{N} |A_{kj}(f)|^2}}, \qquad (2)$$

where A_{ij} represents the autoregressive coefficients, and N is the number of pairwise connections. The frequency bands used for analysis corresponded to the individual RET frequency. The significance connectivity was assessed using bootstrapping method.[30] In our study, the original time series was divided into smaller non-overlapping windows, and the order of these windows was randomly shuffled to create a surrogate time series. Subsequently, a multivariate autoregressive model was fitted to the shuffled time series, and PDC was estimated. This shuffling process was repeated 1000 times. In each run, the group median was calculated, and the 95th percentile of the empirical distribution was then considered as the critical value for significance.

Cross-Frequency Coupling Analysis

Cross-frequency coupling (CFC) refers to the interactions between different frequency bands, and it is believed to play a critical role in various behavioral tasks.[31,32] Power to power is a well-known form of CFC, which demonstrates how amplitude modulations in one frequency depend on the amplitude modulations in another frequency.[33] This coupling can be quantified using the following equation:

$$\mathrm{CFC}_{\text{Power to power}} = \mathrm{corr}\left(a_{f1}[n], a_{f2}[n]\right), \qquad (3)$$

where the Pearson correlation was calculated between the two frequency bands *f1* and *f2*. In this study, the CFC was analyzed between RET frequency originating from the identified connectivity source region and cannonical neuronal activity (alpha:8-13Hz, beta:14-30Hz and gamma: 31-100Hz) from the connectivity sink region.

Statistical Analysis

If not stated otherwise, all analyses were conducted using custom-written R scripts (version 4.2.1). The normality of the data was assessed using the Kolmogorov–Smirnov test. To test for differences

TABLE 1 *Demographics and disease characteristics*

Characteristic	PD, n = 40	HC, n = 40	*P*-value
Mean age, y (SD)	66.78 (5.03)	65.78 (2.72)	0.2722
Handedness (right/left)	37/3	38/2	0.6492
Sex, n (%)			
Male	25 (63)	25 (63)	0.33
Female	15 (37)	15 (37)	
Disease duration, y (SD)	15.25 (2.72)	N/A	
L-Dopa dosage, mg (SD)	916.25 (202.67)	N/A	
UPDRS-III during L-dopa on (SD)	27.35 (4.14)	N/A	
UPDRS-III during L-dopa off (SD)	36.21 (3.82)	N/A	
Resting tremor frequency, Hz (SD)	4.98 (0.77)	3.25 (0.81)	
Re-emergent tremor frequency, Hz (SD)	5.08 (0.83)	3.23 (0.80)	
Tremor rating scale	2.73 (0.91)		

Abbreviations: PD, Parkinson's disease; HC, healthy control; y, year; L-dopa, levodopa; UPDRS-III, Unified Parkinson's Disease Rating Scale part III; (SD), standard deviation.

between levodopa (L-dopa) conditions, *t* tests were performed with Bonferroni adjustment. The statistical significance of P<0.05 was applied to test against the null-hypothesis. Bayesian partial Pearson correlation was used to determine clinical relevance between connectivity and cross-frequency coupling outcomes.[34] We adopted an uninformative prior (uniform distribution) to account for correlations ranging from −1 to +1. This distribution was chosen for correlation with clinical variable including UPDRS-III and L-dopa dosage because the motor examination results and L-dopa effects, particularly in relation to tremor, are relevant and can possibly exhibit varying degrees of correlation with the quantitative measures. Regarding the Hoehn and Yahr scales, which assess disease stage and disability, we anticipate that a reasonable correlation would be in the mild to moderate range, therefore, we have used informative prior distribution and adjusted the width of prior distribution to be narrower covering between −0.75 and +0.75. If the Bayesian factor exceeded 10, we considered it as evidence of correlation. To control false discovery rate (FDR), we used Bayesian FDR control described by Newton and colleagues.[35,36]

Results

Participant Demographics

In this study, the PD group exhibited a mean age of 66.78 ± 5.03 years, which was slightly higher than that of the control group (65.78 ± 2.72 years); however, this difference was not found to be statistically significant ($P > 0.05$). Furthermore, there was no significant difference observed in handedness between the two groups ($P > 0.05$). Regarding clinical characteristics, the PD group demonstrated more pronounced RT and RET frequency as compared to the mimicked RT and RET observed in the control group (Table 1).

Reconstructed Source Locations and the Connectivity Interactions under Medication

Our source analysis revealed differences in brain activity between RT and RET in both PD patients and controls, as shown in Figure 2A. Specifically, PD patients exhibited brain activity in the primary sensorimotor cortex (PSMC), PMC, and CER under L-dopa on condition. However, on withdrawing the medication, PD patients demonstrated source locations in two

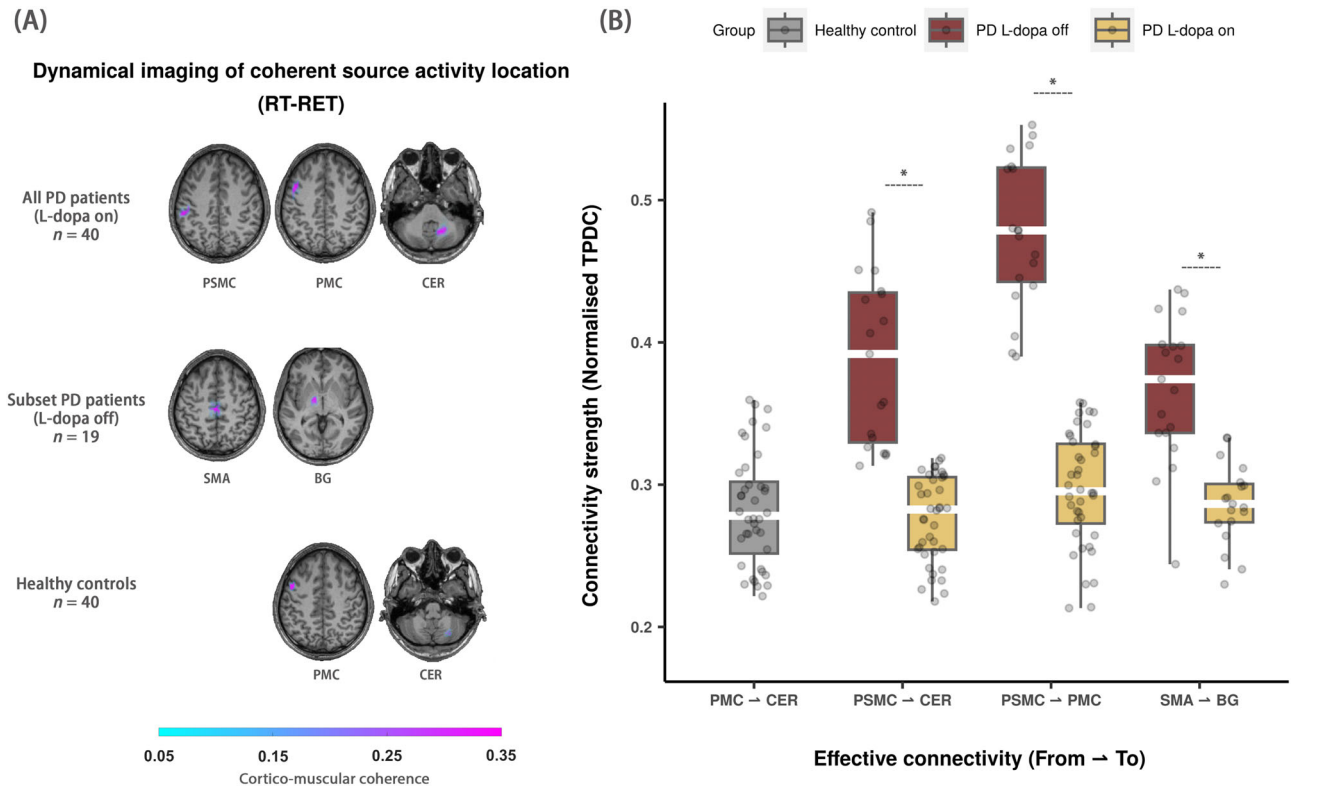

FIG. 2. Coherent source locations and the connectivity interactions. (**A**) Reconstructed coherent source locations contrasted by RT and RET during L-dopa on and off conditions in PD patients and healthy controls. The first row shows the source locations based on all 40 PD patients during L-dopa on. The second row shows the source locations based on 19 PD patients who were measured during L-dopa off. The third row shows the source locations based on 40 healthy controls. (**B**) Boxplot representation of four unidirectional connectivity (statistically significant based on surrogate test), along with their modifications under dopamine medication. BG, basal ganglia; CER, cerebellum; L-dopa, levodopa; PD, Parkinson's disease; PSMC, primary sensorimotor cortex; PMC, premotor cortex; RT, resting tremor; RET, re-emergent tremor; SMA, supplementary motor area; TPDC, time-resolved partial directed coherence. *$P < 0.001$ (Bonferroni adjusted). [Color figure can be viewed at wileyonlinelibrary.com]

brain regions, namely the SMA and the BG region. In contrast, controls showed a similar pattern as PD patients under L-dopa on condition, but without significant activity in the PSMC.

Furthermore, connectivity analysis revealed four statistically significant unidirectional connectivity at individual tremor frequency, as depicted in Figure 2B. These connectivity pairs included PSMC → PMC, PSMC → CER, and SMA → BG among PD patients, and PMC → CER in healthy controls. Notably, PD patients exhibited a higher level of connectivity strength in L-dopa off compared to L-dopa on condition, with PSMC → PMC showing the highest median compared to the other connectivity pairs. After L-dopa administration, PD patients demonstrated reduced connectivity in PSMC → CER ($P < 0.001$), PSMC → PMC ($P < 0.001$), and SMA → BG ($P < 0.001$) compared to L-dopa off condition. Detailed results of the comparison between L-dopa on and off for significant connectivity are summarized in Supplementary Material (Table. S1, Fig. S1,5, Table S9).

Cross-Frequency Coupling and Dopamine Medication Effects

After identifying significant connectivity between the source locations, we performed CFC analysis. This analysis aimed to explore the interaction between RET tremor frequency from the identified connectivity source region, and the canonical neuronal activity from the connectivity sink region, as depicted in Figure 3. Both PD patients and healthy controls showed a

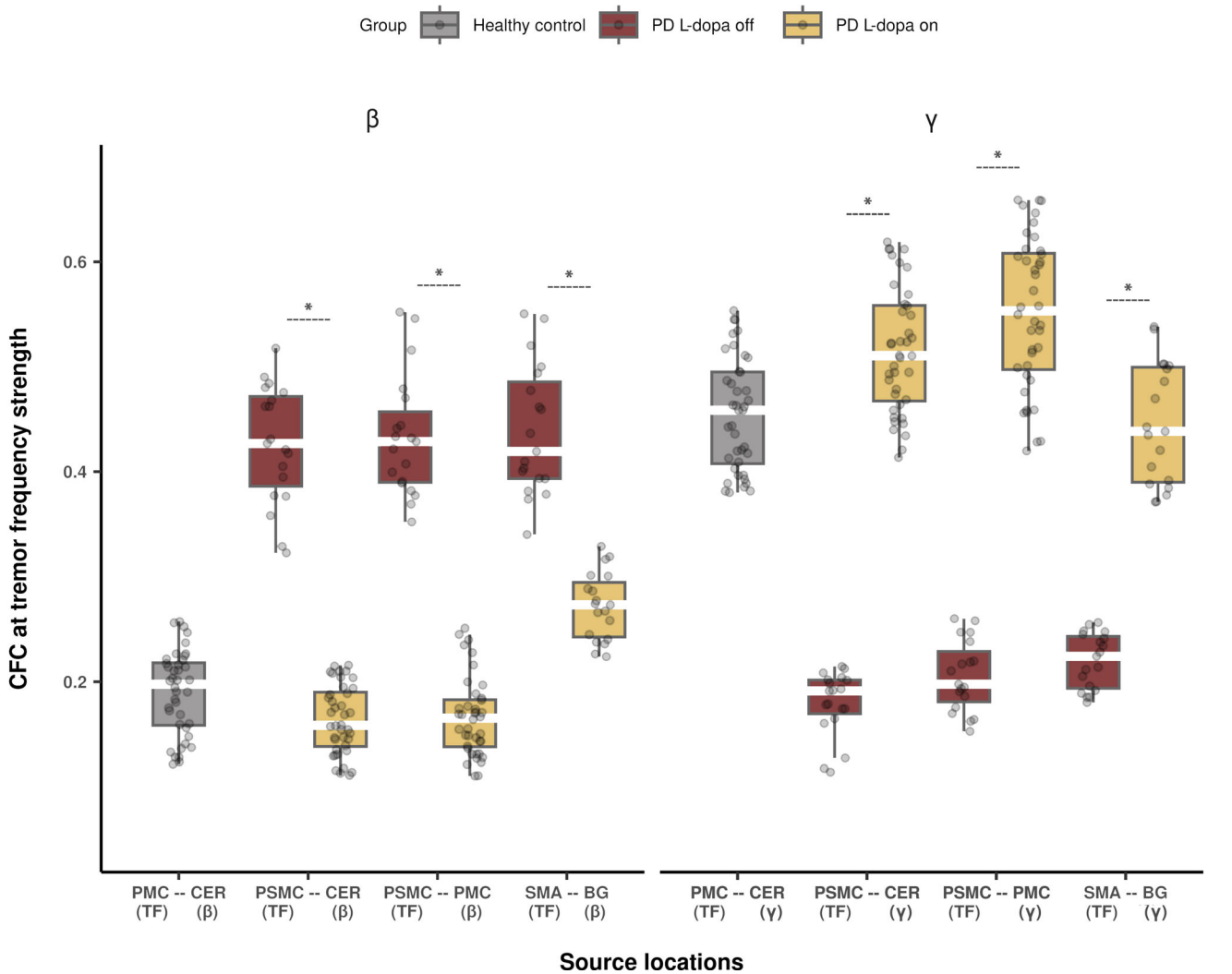

FIG. 3. Cross-frequency coupling between tremor frequency and β/γ oscillations. CFC analysis based on the time series extracted from the difference between RT and RET. The boxplot illustrates the strength of CFC between tremor frequency originating from the connectivity source, and the canonical neuronal activity at the connectivity sink(β/γ) under L-dopa on and off conditions. BG, basal ganglia; CFC, cross-frequency coupling; CER, cerebellum; L-dopa, levodopa; PD, Parkinson's disease; PSMC, primary sensorimotor cortex; PMC, premotor cortex; RT, resting tremor; RET, re-emergent tremor; SMA, supplementary motor area; TF, individual tremor frequency; β, beta frequency band; γ, gamma frequency band. *$P < 0.001$ (Bonferroni adjusted). [Color figure can be viewed at wileyonlinelibrary.com]

tendency of a reversed relationship between β and γ frequency bands from subcortical regions with cortical tremor frequency. In the absence of L-dopa, PD patients exhibited significantly higher cross-frequency coupling strength at β frequency in PSMC-CER ($P < 0.001$), PSMC-PMC ($P < 0.001$), and SMA-BG ($P < 0.001$), but significantly lower coupling strength at γ frequency in PSMC-CER ($P < 0.001$), PSMC-PMC ($P < 0.001$), and SMA-BG ($P < 0.001$) compared to the L-dopa on condition. In healthy controls, the cortical tremor frequency power from PMC coupled with β frequency in CER at a lower level relative to the coupling strength at γ frequency. No difference was observed in power-to-power CFC related to α frequency band (Supplementary Fig. S3). Detailed results of the comparison between L-dopa on and off for CFC are summarized in Supplementary Material (Table S1 and Fig. S2).

Clinical Association with the Strength of Cross-Frequency Coupling and Connectivity

Finally, we investigated the associations between quantified measures and clinical evaluations including UPDRS-III, Hoehn and Yahr scale, and L-dopa dosage. Correlation analysis revealed a positive relationship between L-dopa dosage and effective connectivity in PSMC → PMC ($r = 0.757$, $BF_{10} = 3.481 \times 10^4$) during L-dopa on condition (Fig. 4A). No statistical significance observed in other effective connectivity with the clinical variables. Furthermore, CFC strength between tremor frequency in PSMC and β frequency in CER showed a positive trend with Hoehn and Yahr scale ($r = 0.482$, $BF_{10} = 10.412$). No significant correlations were observed with other clinical measures with CFC (Supplementary Table. S2-8). The detailed Bayesian statistics are summarized in Supplementary Material (Fig. 4).

Discussion

The present study investigated the EEG–EMG coherent source activity between RT and RET. This approach revealed the distinct source locations in the premotor and CER regions in PD patients (L-dopa on) and healthy controls. Using effective connectivity estimation, the study identified exclusive source activity in the PSMC in PD patients, which contribute to the different mechanisms of the two tremor phenotypes. Notably, without dopamine medication, PD patients exhibited a different pattern of source activity in differentiating RT and RET. We further examined the power-to-power cross-frequency coupling between the differential source activity at RET tremor frequency on the connectivity originating regions and β and γ oscillations on the connectivity sink regions during L-dopa on and off conditions. The results revealed that dopamine medication can influence the coupling between the

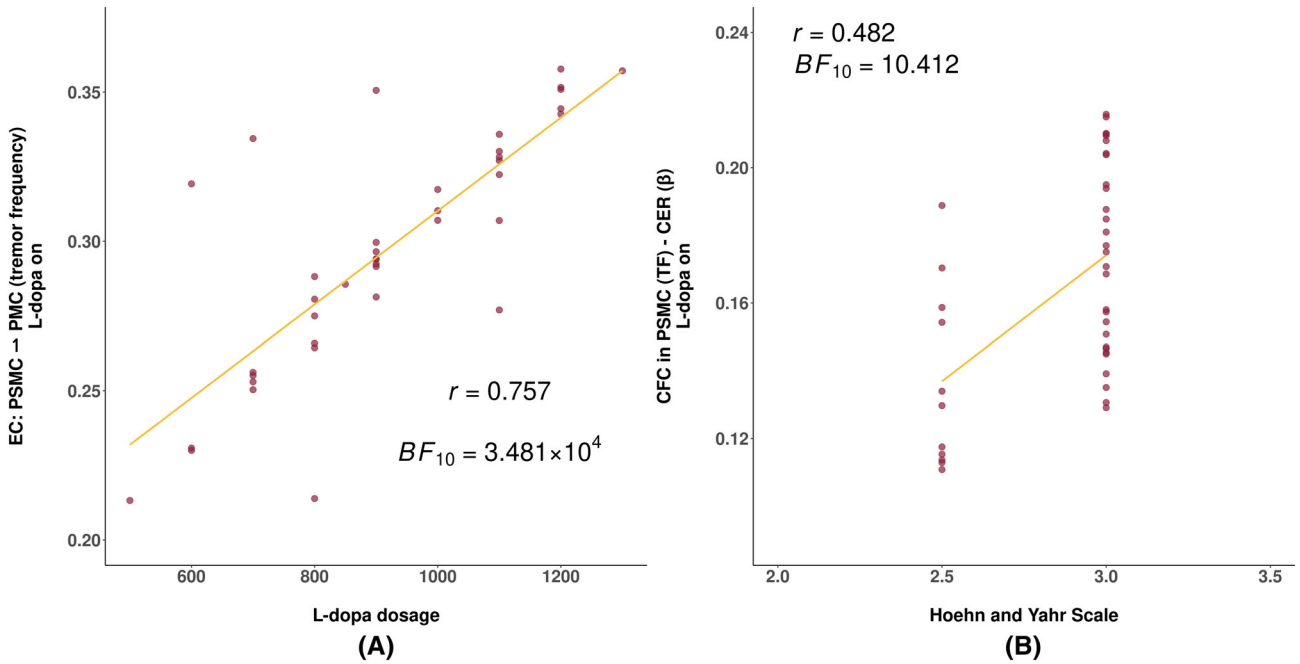

FIG. 4. Bayesian partial correlation analysis between clinical measures and both the strength of cross-frequency coupling and connectivity in PD patients. (**A**) Positive correlation between L-dopa dosage and effective connectivity in PSMC → PMC during L-dopa on condition. (**B**) Positive correlation between Hoehn and Yahr scale and the CFC strength between cortical tremor frequency from PSMC and β frequency from CER during L-dopa on. CER, cerebellum; CFC, cross-frequency coupling; L-dopa, levodopa; PSMC, primary sensorimotor cortex; PMC, premotor cortex; *r*, partial correlation coefficient. BF_{10} Bayesian factor under alternative hypothesis (False discovery rate < 0.05). [Color figure can be viewed at wileyonlinelibrary.com]

tremor frequency and β and γ activity. These findings imply the presence of discernable neural activity patterns distinguishing RT from RET, evidencing the impact of dopamine medication and the tremor associated neural characteristics of beta and gamma activity.

Previous studies have suggested that RET shares the same central tremor circuit as RT and may be an extension of it.[6] Although, our current study identified different coherent sources between the two tremor phenotypes, the contrast between RT and RET demonstrated consistent strength in cortico-muscular coherence from each source, thus confirming this assumption. Both PD patients (L-dopa on) and healthy controls exhibited significantly difference of source activity in the PMC and CER regions, which are known to play crucial roles in tremor circuits. Specifically, the PMC is involved in the central representation of RT, whereas the CER plays a modulator role.[12]

Both PMC and CER were found to be involved in motor imagery[37] and have been implicated in the pathophysiology of tremor.[11] In the context of RT, the lack of voluntary movement may result in the overactivity in the PMC and CER. Moreover, RET may involve sensory feedback generated by repositioning the limb from a resting to an outstretched posture. This feedback could increase somatosensory input and produce reverberations within the cerebello-thalamo-cortical tremor circuit,[1] potentially reducing the need for modulation in the PMC and CER. This could explain the lower levels of source activity observed in these regions during RET compared to RT.

Interestingly, PSMC was found to play a role in tremor phenotypes in PD patient. This region is known responsible for sensory processing and its involvement in tremor has been reported in previous studies.[10,38] Effective connectivity further revealed the unidirectional flow from the PSMC to both the PMC and CER, suggesting a key role of PSMC as potential modulator within the cortico-subcortical interaction in PD. Furthermore, these two PSMC related connections showed an association with Levodopa dosage and disease stages during L-dopa on condition, indicating this brain region as a crucial component in the disease pathology and tremor circuit such as cerebello-thalamo-cortical loop in PD patients. This aligns with the reported functional reorganization of the sensorimotor cortex associated with PD,[39] which may reflect either compensatory changes or maladaptive plasticity in response to abnormal BG activity that affects to sensorimotor and its associated cortical areas.[40] Moreover, the strength of the connectivity related to PSMC decreased after the medication. One possible explanation is that L-dopa could partially normalize the connectivity of the BG motor circuit,[41] leading to a reduction in the cortico-cerebellar loop. Consequently, the flow of information from the PSMC to the CER may have been attenuated.

In addition, the observed coherent source activity during L-dopa off condition revealed another neural circuitry between RT and RET in PD patients. Specifically, the coherent source activity exhibited a distinct pattern (SMA and BG) compared to the L-dopa on condition (PSMC, PMC, and CER) and the tremor pattern seen in healthy controls (PMC and CER). A previous study suggested that the SMA plays a crucial role in parkinsonian tremor and is coupled with other motor areas with pathologically synchronized activity.[12] Meanwhile, the subthalamic nucleus may be involved in triggering tremor through its connectivity with the globus pallidus internus and in maintaining the tremor rhythm.[7] One possible explanation for the distinct pattern during L-dopa off condition is that because of insufficient dopamine levels as input to the striatum, RET may depend less on the BG circuitry, but more on the cerebello-thalamo-cortical circuit. This may also explain a previous finding by Helmich and colleagues[9] that transcranial magnetic stimulation at CER can reset RET, but not RT. It might also support why RET is less responsive to L-dopa in some studies,[6] because it involves non-dopaminergic areas such as the CER.

Previous studies highlighted cortical regions such as primary motor cortex as a key role in controlling tremor amplitude,[8,9] and its wide network with other cortical regions within cortico-thalamo-cerebellar loop involved in the pathophysiology of tremor in PD.[12] In the current study, cross-frequency coupling revealed the involvement of β and γ oscillations in tremor phenotypes and oscillatory modifications related to dopamine level. As the time series of each source activity already represented the difference between two tremor phenotypes, our findings first demonstrated there is a difference of power in the frequency domain. Although a few studies reported no difference in mean frequency between RT and RET,[5,42] several studies showed a visible higher frequency and peak power of RET compared to RT.[6,7,9] Second, the mimicked tremor from healthy controls exhibited frequency coupling between tremor frequency from PMC with β power from the CER, at a relatively lower level, in contrast to γ frequency. This suggests that there is a hypoactive γ oscillatory modulation involved in the differential circuitry between RT and RET in PD. Similarly, PD patients could attain the same degree of coupling in the cortico-subcortical network through the PSMC (PSMC – PMC and PSMC – CER) under the influence of dopamine medication. This observation is consistent with studies on the oscillatory profile of the sensorimotor cortex in PD, which may aid in facilitating movement to counteract the antikinetic bias induced by the dopamine-depleted state.[43] In our dataset, we identified a positive correlation between the Hoehn and Yahr scale and CFC within the β band. If an enhanced neural oscillatory coupling between tremor frequency and pathological β activity

indeed influences tremor phenotypes and serves as a reflection of disease severity, it is plausible that the presence of PSMC in PD might play a compensatory role within this network. On withdrawal of L-dopa, there was a significant increase in the coupling strength between the SMA and BG. This distinct pattern observed in PD patients may be caused by the alteration in the basal ganglia-thalamo-cortico network, which can lead to prominent β oscillations in the BG.[44] In CFC, a higher level of oscillatory coupling between tremor frequency from SMA and β oscillations from BG indicates the importance of β modulation in the mechanism of RT and RET. Nevertheless, the coupling strength does not decline to the same extent as other regions under the L-dopa on condition, implying that dopamine medication may have relatively limited effect on modulating tremor-related β power between the SMA and BG regions.

One limitation of this study is that although we have identified several source locations, we cannot exclude the possible effects of anatomical distribution variations of tremors on the activity. Since frequency coupling analysis does not provide directional information, we were unable to determine the directionality of oscillatory interactions in our study. Instead, we relied on the individual tremor frequency of the cortical source. This approach is based on empirical findings that tremor amplitude is associated with cortical activity. To address this issue, future studies could consider the utilization of other methods to examine the directional information of the oscillatory interactions. It is important to note that our study focused on a relatively homogenous cohort by excluding advanced PD patients (Hoehn and Yahr scale >4). The deliberate exclusion of advanced PD patients was motivated by our aim to conduct a more targeted investigation into the neural activity patterns associated with RT and RET within a controlled context. This approach allowed us to uncover specific insights without the potential confounding factors introduced by the varied manifestations of advanced PD. Future studies may consider the inclusion of advanced PD patients to explore the continuum of tremor manifestations across different disease stages. Such investigations could provide valuable insights into the progression of neural changes associated with tremor in PD, contributing to a more comprehensive understanding of the disorder. Parkinsonian tremor and voluntarily mimicked tremor represent fundamentally different motor phenomena; however, magnetoencephalographic and imaging data suggest their origin in the same motor centers of the brain.[45,46] This forms the basis for the interference of pathological tremor oscillations with voluntary movements.[47] Nevertheless, questions persist regarding how the difference between voluntarily controlled movements and the self-sustained pathological tremor oscillations of PD is manifested in this motor network. A plausible explanation is that altered cortical–subcortical communications impact the thalamocortical loop, which plays a fundamental role distinguishing PD from mimicked tremor.[11] In this study, our findings support this assumption, because the engagement of the PSMC in tremor phenotypes was exclusively observed in PD. However, the role of PSMC during RET remains a topic for future research.

In conclusion, the current study has provided evidence for distinctive patterns of neural activity between RT and RET, indicating distinct mechanisms of tremor modulation within the cortico-subcortical network. During RT, the PSMC may act as a primordial modulator between the PMC and the CER, mitigating the effects of BG circuit dysfunction in the absence of voluntary movement. Conversely, in RET, PD patients may rely less on the BG circuit and more on the cerebello-thalamo-cortical pathway. Moreover, the oscillatory neuronal responses provide direct evidence of pathological β and prokinetic γ activity in patients between RT and RET. These discoveries play a fundamental role in advancing our understanding of tremor phenomena and its therapeutic modulation through the administration of dopamine medication or the application of deep brain stimulation, which could specifically target the pathological β and prokinetic γ oscillations related to tremor and motor control. ■

Acknowledgments: We extend our gratitude to all participants who participated in this study. We also express our gratitude to Miss Meng Shi for her invaluable advice in graphic design for the manuscript. The authors declare that there are no conflicts of interest relevant to this work. Open Access funding enabled and organized by Projekt DEAL.

Data Availability Statement

The data that support the findings of this study are available from the corresponding author, upon reasonable request.

References

1. Dirkx MF, Bologna M. The pathophysiology of Parkinson's disease tremor. J Neurol Sci 2022;435:120196.
2. Lenka A, Jankovic J. Tremor syndromes: an updated review. Front Neurol 2021;12:684835.
3. Muthuraman M, Schnitzler A, Groppa S. Pathophysiology of tremor. Nervenarzt 2018;89(4):408–415.
4. Deuschl G, Papengut F, Hellriegel H. The phenomenology of parkinsonian tremor. Parkinsonism Relat D 2012;18:S87–S89.
5. Jankovic J, Schwartz KS, Ondo W. Re-emergent tremor of Parkinson's disease. J Neurol Neurosurg Psychiatry 1999;67(5):646.
6. Dirkx MF, Zach H, Bloem BR, et al. The nature of postural tremor in Parkinson disease. Neurology 2018;90(13):e1095–e1103.
7. Helmich RC. The cerebral basis of parkinsonian tremor: a network perspective. Mov Disord 2018;33(2):219–231.
8. Leodori G, Belvisi D, Bartolo MID, et al. Re-emergent tremor in Parkinson's disease: the role of the motor cortex. Mov Disord 2020; 35(6):1002–1011.

9. Helmich RC, Berg KREV d, Panyakaew P, et al. Cerebello-cortical control of tremor rhythm and amplitude in Parkinson's disease. Mov Disord 2021;36(7):1727–1729.
10. Muthuraman M, Raethjen J, Koirala N, et al. Cerebello-cortical network fingerprints differ between essential, Parkinson's and mimicked tremors. Brain J Neurol 2017;141(6):1770–1781.
11. Muthuraman M, Heute U, Arning K, et al. Oscillating central motor networks in pathological tremors and voluntary movements. What makes the difference? Neuroimage 2012;60(2):1331–1339.
12. Timmermann L, Gross J, Dirks M, et al. The cerebral oscillatory network of parkinsonian resting tremor. Brain 2003;126(1):199–212.
13. Lauro PM, Lee S, Akbar U, Asaad WF. Subthalamic-cortical network reorganization during Parkinson's tremor. J. Neurosci Off J Soc 2021;41(47):9844–9858.
14. Hughes AJ, Daniel SE, Kilford L, Lees AJ. Accuracy of clinical diagnosis of idiopathic Parkinson's disease: a clinico-pathological study of 100 cases. J Neurol Neurosurg Psychiatry 1992;55(3):181.
15. Hoehn MM, Yahr MD. Parkinsonism onset, progression, and mortality. Neurology 1967;17(5):427.
16. Journee HL. Demodulation of amplitude modulated noise: a mathematical evaluation of a demodulator for pathological tremor EMG's. IEEE T Bio-med Eng 1983;30(5):304–308.
17. Welch P. The use of fast Fourier transform for the estimation of power spectra: a method based on time averaging over short, modified periodograms. IEEE Trans Audio Electroacoustics 1967;15(2):70–73.
18. Halliday DM, Rosenberg JR, Amjad AM, et al. A framework for the analysis of mixed time series/point process data—theory and application to the study of physiological tremor, single motor unit discharges and electromyograms. Prog Biophys Mol Biol 1995; 64(2–3):237–278.
19. Mitra PP, Pesaran B. Analysis of dynamic brain imaging data. Biophys J 1999;76(2):691–708.
20. Muthuraman M, Galka A, Deuschl G, et al. Dynamical correlation of non-stationary signals in time domain—a comparative study. Biomed Signal Proces 2010;5(3):205–213.
21. Amjad AM, Halliday DM, Rosenberg JR, Conway BA. An extended difference of coherence test for comparing and combining several independent coherence estimates: theory and application to the study of motor units and physiological tremor. J Neurosci Methods 1997;73(1):69–79.
22. Rosenberg JR, Amjad AM, Breeze P, et al. The Fourier approach to the identification of functional coupling between neuronal spike trains. Prog Biophys Mol Biol 1989;53(1):1–31.
23. Sekihara K, Scholz B. Generalized wiener estimation of three-dimensional current distribution from biomagnetic measurements. IEEE Transactions Bio-Med Eng 1996;43(3):281–291.
24. Gross J, Ioannides AA. Linear transformations of data space in MEG. Phys Med Biol 1999;44(8):2081–2097.
25. Veen BDV, Drongelen WV, Yuchtman M, Suzuki A. Localization of brain electrical activity via linearly constrained minimum variance spatial filtering. IEEE T Bio-Med Eng 1997;44(9):867–880.
26. Muthuraman M, Bange M, Koirala N, et al. Cross-frequency coupling between gamma oscillations and deep brain stimulation frequency in Parkinson's disease. Brain 2020;143(11):awaa297.
27. Bourguignon M, Piitulainen H, Tiège XD, et al. Corticokinematic coherence mainly reflects movement-induced proprioceptive feedback. Neuroimage 2015;106:382–390.
28. Wan EA, Nelson AT. Dual extended Kalman filter methods. Kalman Filter Neural Netw 2001;123-173.
29. Baccalá LA, Sameshima K. Partial directed coherence: a new concept in neural structure determination. Biol Cybern 2001;84(6):463–474.
30. Kamiński M, Ding M, Truccolo WA, Bressler SL. Evaluating causal relations in neural systems: granger causality, directed transfer function and statistical assessment of significance. Biol Cybern 2001; 85(2):145–157.
31. Jirsa V, Müller V. Cross-frequency coupling in real and virtual brain networks. Front Comput Neurosc 2013;7:78.
32. Jafakesh S, Jahromy FZ, Daliri MR. Decoding of object categories from brain signals using cross frequency coupling methods. Biomed Signal Proces 2016;27:60–67.
33. Davoudi S, Ahmadi A, Daliri MR. Frequency–amplitude coupling: a new approach for decoding of attended features in covert visual attention task. Neural Comput App 2021;33(8):3487–3502.
34. Kucharský Š, Wagenmakers E-J, van den Bergh D, Ly A. Analytic posterior distribution and bayes factor for pearson partial correlations; 2023.
35. Newton MA, Noueiry A, Sarkar D, Ahlquist P. Detecting differential gene expression with a semiparametric hierarchical mixture method. Biostatistics 2004;5(2):155–176.
36. Newton JM, Sunderland A, Gowland PA. fMRI signal decreases in ipsilateral primary motor cortex during unilateral hand movements are related to duration and side of movement. Neuroimage 2005; 24(4):1080–1087.
37. Taube W, Mouthon M, Leukel C, et al. Brain activity during observation and motor imagery of different balance tasks: an fMRI study. Cortex 2015;64:102–114.
38. Playford ED, Jenkins IH, Passingham RE, et al. Impaired mesial frontal and putamen activation in Parkinson's disease: a positron emission tomography study. Ann Neurol 1992;32(2):151–161.
39. Kojovic M, Bologna M, Kassavetis P, et al. Functional reorganization of sensorimotor cortex in early Parkinson disease. Neurology 2012;78(18):1441–1448.
40. Milardi D, Quartarone A, Bramanti A, et al. The Cortico-basal ganglia-cerebellar network: past, present and future perspectives. Front Syst Neurosci 2019;13:61.
41. Gao L, Zhang J, Chan P, Wu T. Levodopa effect on basal ganglia motor circuit in Parkinson's disease. CNS Neurosci Ther 2017; 23(1):76–86.
42. Bellows S, Jankovic J. Parkinsonism and tremor syndromes. J Neurol Sci 2022;433:120018.
43. Rowland NC, Hemptinne CD, Swann NC, et al. Task-related activity in sensorimotor cortex in Parkinson's disease and essential tremor: changes in beta and gamma bands. Front Hum Neurosci 2015;9:512.
44. Wingeier B, Tcheng T, Koop MM, et al. Intra-operative STN DBS attenuates the prominent beta rhythm in the STN in Parkinson's disease. Exp Neurol 2006;197(1):244–251.
45. Pollok B, Gross J, Dirks M, et al. The cerebral oscillatory network of voluntary tremor. J Physiol 2004;554(3):871–878.
46. Parker F, Tzourio N, Blond S, et al. Evidence for a common network of brain structures involved in parkinsonian tremor and voluntary repetitive movement. Brain Res 1992;584(1–2):11–17.
47. Raethjen J, Pohle S, Govindan RB, et al. Parkinsonian action tremor: interference with object manipulation and lacking levodopa response. Exp Neurol 2005;194(1):151–160.

Supporting Data

Additional Supporting Information may be found in the online version of this article at the publisher's web-site.